EVALUATION OF CLAY CONSTITUTIVE MODELS FOR ANALYSIS OF DEEP EXCAVATION UNDER UNDRAINED CONDITIONS

Aswin Lim [1], Chang-Yu Ou [2], and Pio-Go Hsieh [3]

ABSTRACT

The objective of this study is to evaluate the performance of the most commonly used constitutive models of clay for analysis of deep excavation under the undrained condition. Five soil models, *i.e.*, the modified Cam clay model, the hardening soil model, the hardening soil small strain model, the Mohr-Coulomb ($\phi = 0$) and the undrained soft clay model, are selected for evaluation. The TNEC excavation case history, which was with well-documented monitoring data and soil properties, is used for this purpose. Results indicate that the modified Cam Clay model, with a raise of the κ/λ ratio to 0.2 ~ 0.25 for normally consolidated clay and without adjustment of κ/λ ratio for overconsolidated clay, can yield predicted wall deflections close to field measurements for the final stage of excavation. The hardening soil model and hardening soil small strain model with the parameters directly obtained from tests can yield wall deflections close to field measurements for the final stage of excavation. The $\phi = 0$ Mohr-Coulomb model with $E_u/s_u = 500$ can result in good prediction for wall deflections for final stage of excavation. None of those four soil models can predict good ground settlement profiles. The undrained soft clay model with the parameters directly from tests can predict both wall deflections and surface settlements well.

Key words: Deep excavation, MCC model, HS model, HS small model, Mohr-Coulomb model, USC model.

1. INTRODUCTION

In geotechnical engineering, there are two concepts for analyzing undrained geotechnical problems, which are the effective stress analysis and the total stress analysis. In the effective stress analysis water and soil are treated separately, but in the total stress analysis water and soil are treated as a single material. These two concepts can be approached with soil models that have been developed by many researchers. In practice, engineers more like using the total stress soil model to analyze undrained problems instead of the effective stress soil model because soil parameters of the total stress soil model are more familiar and easier to be obtained with conventional soil tests. Effective stress soil models are more preferred by scientists because this type of soil models is with more solid theoretical formulation.

In the effective stress approach, there are several soil models that have been used in geotechnical analyses, such as the modified Cam Clay model (MCC model), hardening soil model (HS model), the hardening soil small strain model (HS small model). The MCC model (Burland 1965) was firstly derived following the critical state soil mechanics theory. The HS model (Schanz *et al*. 1999) and the HS-small model (Benz *et al*. 2009) are based on hardening rule and quite popular in recent years. These three soil models are rather simpler than advance soil models and many commercial softwares like PLAXIS, FLAC, and so on have been implemented with those soil models. However, neither of those models can fully simulate the real soil behavior because the shape of the yield locus is assumed to be symmetric to the hydrostatic axis. Moreover, recently developed advanced soil models in the literature like MIT E3 (Hashash and Whittle 1996) and MIT S1 models (Pestana and Whittle 1999) need more soil parameters that are not easily to be obtained from conventional soil tests.

In the total stress soil model approach, the stress and constitutive soil models are expressed in terms of total stress. However, according to the effective stress principle, the soil behavior is governed by effective stress rather than total stress. Therefore, the parameters for this type of models should consider the development of pore water pressure and influence of stress history, that is, the principle of effective stress should be implicitly defined in the parameters. Otherwise, the parameters are often determined with empirical correlations. There are several soil models that are approached with the total stress such as the Mohr-Coulomb model ($\phi = 0$) and the undrained soft clay model (USC model). The $\phi = 0$ Mohr-Coulomb model is a traditional and widely used in geotechnical research as well as in industry purpose and the USC model is newly developed soil model (Hsieh *et al*. 2010).

Though the MCC model, HS model, HS small model, and the $\phi = 0$ Mohr-Coulomb model have been implemented into some of the commonly used softwares, few of them in literature are studied in relative to field measurements. Hence, this study aims to evaluate the performance of those models. It is expected that the evaluation can be helpful to engineers and researchers to perform analysis using those models more confidently.

Evaluation of the performance of the above mentioned models requires good case histories. The Taipei National Enterprise Center (TNEC) excavation is one of good excavation cases that field monitoring data and soil testing data were recorded well and complete (Ou *et al*. 1998, 2000a, and 2000b). Also, new soil tests on the soil at the construction site were recently conducted to check the consistency of soil parameters. With the new soil data, the soil data were upgraded and the determination of input parameters become assuredly.

Manuscript received March 8, 2010; revised April 7, 2010; accepted April 8, 2010.

[1] Graduate student, Department of Construction Engineering, National Taiwan University of Science and Technology, Taiwan 10672, R.O.C.

[2] Professor (corresponding author), Department of Construction Engineering, National Taiwan University of Science and Technology, Taipei, Taiwan 10672, R.O.C. (e-mail: ou@mail.ntust.edu.tw).

[3] Professor, Department of Assets and Property Management, Hwa Hsia Institute of Technology, Taipei, Taiwan 23568, R.O.C. (e-mail: spg@cc.hwh.edu.tw).

2. THE TAIPEI NATIONAL ENTERPRISE CENTER (TNEC) CASE HISTORY

The TNEC structure is an 18 story building with five level basements. The depth of the excavation was 19.7 m, with dimension of diaphragm wall was 90 cm thick and 35 m deep. The groundwater level was at a depth of 2.0 m below the ground surface (GL−2.0 m). The excavation was completed in seven stages. Figure 1 shows the sequence of excavation and basement construction.

According to site investigation, stratigraphic condition at the site can be described as follows (Fig. 1): The first layer is soft silty clay (CL), which ranges from ground surface level (GL) 0.0m to GL−5.6 m and whose N-value is around 2 ~ 4. The second layer, from GL−5.6 m to GL−8.0 m, loose silty fine sand with N-values between 4 ~ 11 and $\phi' = 28°$. The third layer, from GL−8.0 m to GL−33.0 m, is again soft silty clay (CL) whose N-value is around 2 ~ 5 and the PI is within the range of 9 ~ 23, with an average value of 17. This layer is the one which most affects excavation behavior. The fourth layer, ranging from GL−33.0 m to GL−35.0 m, is medium dense silty fine sand with N-value between 22 and 24 and $\phi' = 32°$. The fifth layer is medium soft clay, ranges from GL−35.0 m to GL−37.5 m, N-value between 9 ~ 11. The sixth layer is medium dense to dense silt or silty fine sand; ranges from GL−37.5 m to GL−46.0 m, N = 14 ~ 37 and $\phi' = 32°$. Below the sixth layer is dense Chingmei gravel soil and N is above 100.

Figure 2 shows the variation of water content and in-situ void ratio with depth obtained from Ou *et al*. (1998), along with the test data conducted recently (Teng 2010). Figure 3 shows the values of compression index and swelling index obtained from Ou *et al*. (1998), along with the test data conducted recently. Figure 4(a) shows the variation of OCR with depth. As shown in the figure, the clay at depths of below 12 m (*i.e.*, GL−12) can be treated as the normally consolidated clay and above GL−12m are overconsolidated. Figure 4(b) shows the variation of undrained shear strength obtained from the UU test, the field vane shear test and CK_0U-*AC* test and CK_0U-*AE* test and with new test data conducted recently (Teng 2010).

3. ANALYSIS AND DISCUSSION

In this study, the computer program, PLAXIS, was used for evaluation. In the analysis, the stiffness of structural parameters is reduced by 20% from the nominal value, considering that the stiffness of the concrete retaining wall reduces when large bending moment of the diaphragm wall causes the occurrence of the crack in the concrete. The axial stiffness of the temporary steel struts and concrete floor slab are reduced by 20%. Table 1 lists the structural properties used for analysis.

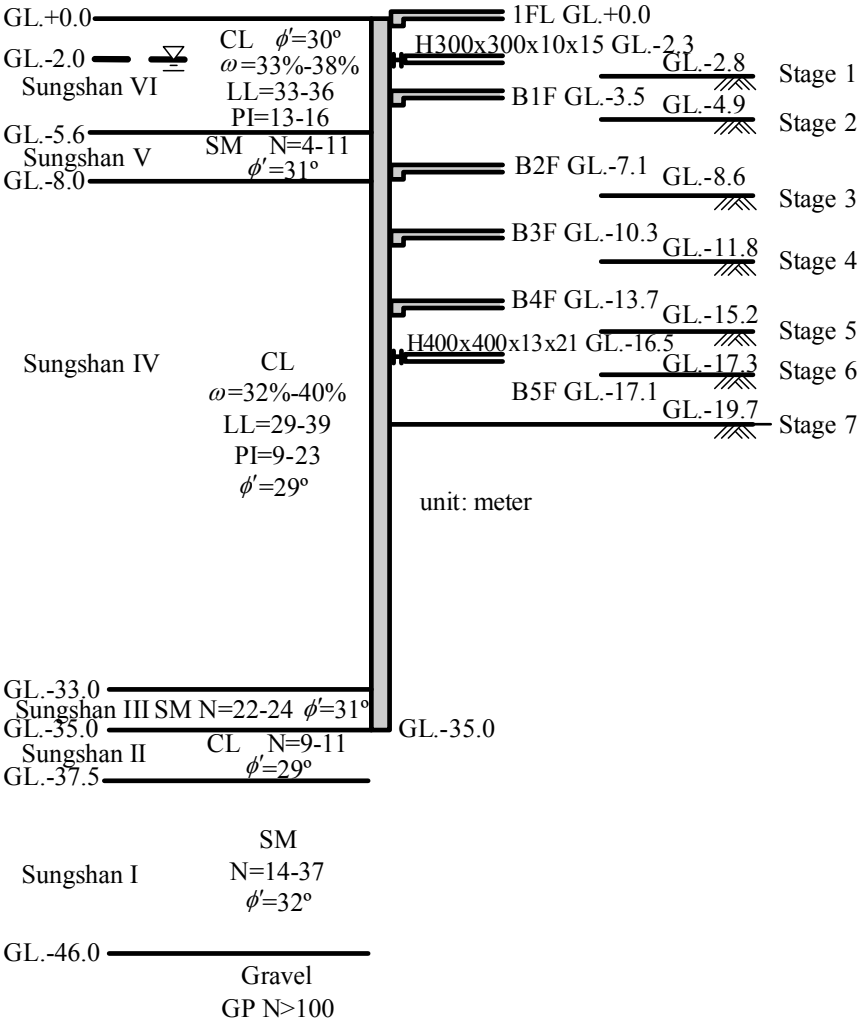

Fig. 1 Profile of excavation sequence and subsurface soil layers

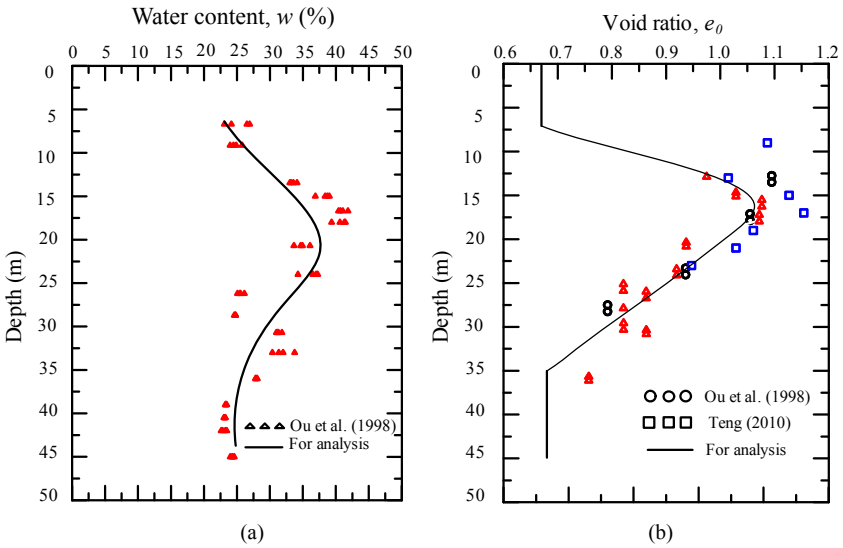

Fig. 2 The variation of (a) water content and (b) initial void ratio with depth

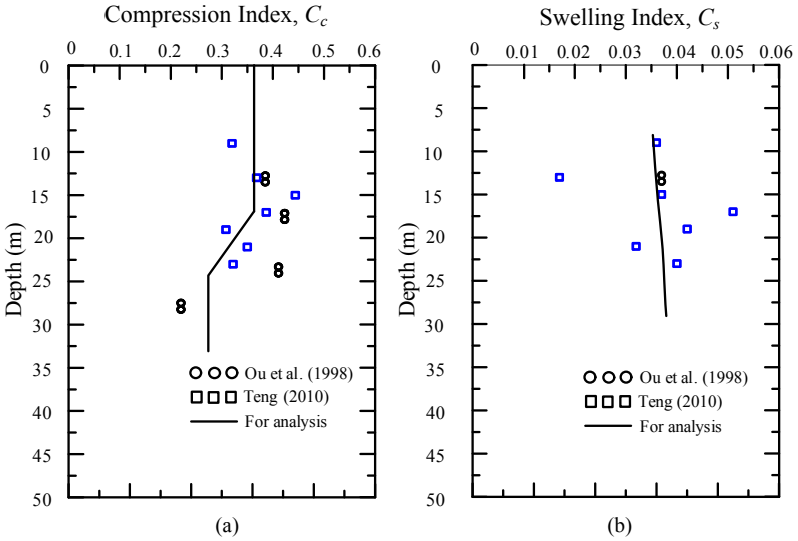

Fig. 3 The variation of (a) compression index and (b) swelling index with depth

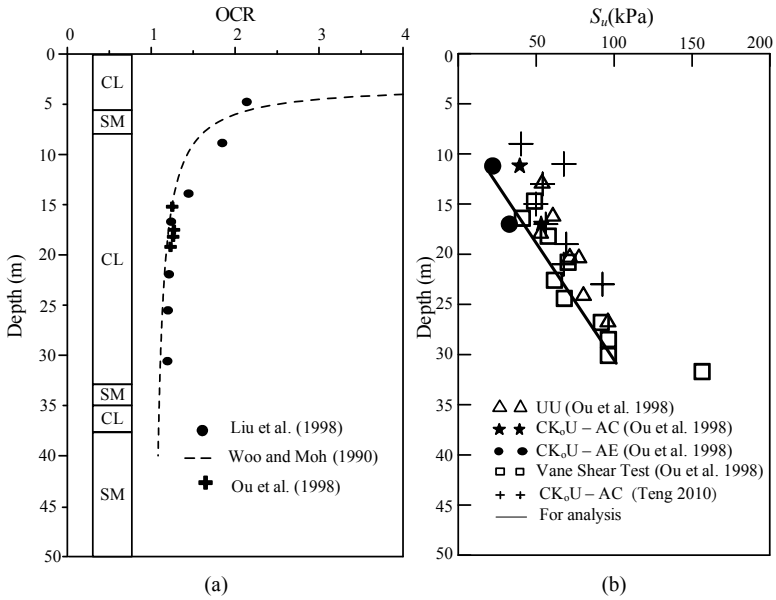

Fig. 4 The variation of (a) OCR and (b) undrained shear strength with depth

Table 1 Input parameters for the lateral support

Stage	Type	A (m^2)	t (m)	s (m)	E (MPa)	υ
1	steel	0.012	–	8	210000	0.2
2	slab	–	0.15	–	21000	0.15
3	slab	–	0.15	–	21000	0.15
4	slab	–	0.15	–	21000	0.15
5	slab	–	0.15	–	21000	0.15
6	steel	0.0219	–	3.4	210000	0.2

Note: s = spacing distance between struts; t = thickness of slab

Table 2 Input parameters of drained material for the Mohr-Coulomb model

Depth (m)	N_{design}	γ (kN/m^3)	ϕ′ (deg)	E (kPa)	υ
5.6 ~ 8	7	18.93	30	68351	0.3
33 ~ 35	23	19.62	33	265473	0.3
37.5 ~ 45	26	19.62	35	300247	0.3

Note:
(1) N is the standard penetration number adopted from Fig. 1
(2) E is the Young's modulus and is a function of N

Since clay, locating at depths of GL−8 m and GL−33 m, is a predominant soil which affects excavation behavior, the clay is simulated as an undrained material using the MCC model, the HS model, the HS small model, and the $\phi = 0$ Mohr-Coulomb model. To be consistent, all sand layers are simulated as a drained material using the Mohr-Coulomb model.

With the Mohr-Coulomb effective drained analysis, the input parameters are effective soil cohesion (c'), effective angle of soil friction (ϕ'), effective Young's modulus of soil (E), and effective Poisson's ratio (υ). Values of ϕ' were obtained from the direct shear test, as described in the preceding section and υ can be set equal to 0.3 according to the suggestion in the PLAXIS manual. According to Ou and Lai (1994), the E value was obtained from the following equation:

$$E = 2 \times \beta \times G(1+\upsilon) \tag{1}$$

where G is the shear modulus, $G = \rho V_s^2$; ρ is the density of soil, V_s is the shear wave velocity and can be estimated through the wave equation, *i.e.*, relationship between V_s and the standard penetration number (N); β is a reduction factor which considers the difference between small strain and the strain at the normal condition and the β value can be set equal to 0.5 based on many experience (Ou 2006). Table 2 lists the input parameters of drained material used for analysis.

Figure 5 shows the finite element mesh used for analysis, in which the left boundary is set a the center of excavation, considering the symmetry of the excavation, the right boundary at a distance of 100 m from the excavation center, which is beyond the excavation influence zone, usually larger than 4 times excavation depth and the bottom at the gravel soil level, *i.e.*, 45 m below the surface. The left and right vertical boundaries are restrained from the horizontal movement and the bottom is restrained from both the vertical and horizontal movements.

3.1 The Modified Cam-Clay Model

The modified cam-clay model (Burland 1965) was modification in flow rule from original cam-clay model (Schofield and Worth 1968). This model is based on the critical state theory and was originally meant to simulate the behavior of normally and near-normally consolidated clays under triaxial compression test conditions. The yield surface of modified Cam Clay model in the p-q stress space is ellipse in shape and symmetric with respect to the hydrostatic line. The modified Cam-clay constitutive model involves five parameters, *i.e.*, the frictional constant, M, the isotropic logarithmic compression index, λ, the swelling index, κ, pure elastic or unloading-reloading Poisson's ratio, υ_{ur}, and pure elastic or unloading-reloading Young's modulus, E_{ur}.

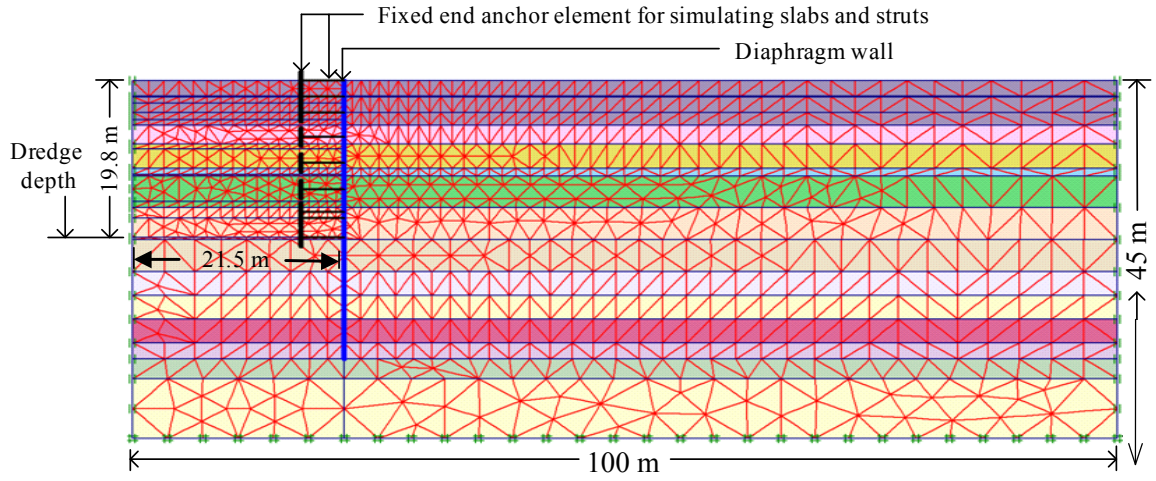

Fig. 5 Finite element mesh of the TNEC case used for analysis

The frictional parameter, M, is function of ϕ', where $M = (6\ \sin\phi' / 3\ -\sin\phi')$. The logarithmic compression index, λ, is equal to C_c /2.303 and swelling index, κ, is equal to C_s /2.303 where C_c the compression index and C_s is the swelling index. As shown in Fig. 3, the ratio of C_s / C_c or κ / λ is about 0.09 ~ 0.15 and the solid line is selected for analysis. The pure Poisson's ratio can be assumed to be 0.2 as suggested in the PLAXIS manual. Since behavior along a swelling line, whose equation is $e + \kappa(\ln p) = e_s$ where e_s is the void ratio when $p = 1$, the pure elastic volumetric strain can be determined from the derivative of the swelling line equation as

$$d\varepsilon_v^e = \frac{de}{1+e} = \frac{\kappa}{1+e}\frac{dp}{p} \tag{2}$$

The elastic or unloading/reloading bulk modulus can then be derived as

$$K_{ur} = \frac{dp}{d\varepsilon_v^e} = \frac{(1+e)p}{\kappa} \tag{3}$$

The elastic Young's modulus at the reference pressure, p, can be determined as

$$E_{ur} = 3K_{ur}(1-2\upsilon_{ur}) = \frac{3(1+e)\,p(1-2\upsilon_{ur})}{\kappa} \tag{4}$$

Therefore, given the value of e, κ, υ_{ur}, and the current stress state p, the elastic Young's modulus can be obtained through Eq. (4). Table 3 lists the input parameters of undrained material for the MCC constitutive model used for analysis. Figure 6 shows the comparison of measured wall displacements and those predicted using the MCC model with the parameters directly from the laboratory tests, that is, real soil parameter. As shown in the figure, the wall displacements are close to field measurement at early stages (stages 1 and 2) while the predicted wall deflections are smaller than the field measurements for intermediate to final stages. This can be explained by the fact that the MCC yield surface is symmetric to the hydrostatic line and the real soil yield surface is symmetric to the about K_0 line (Fig. 7). At the early stages, the soil is subjected to small unloading force, causing the stress state to be the inside of the MCC yield surface, and meanwhile also the inside of the real soil yield surface. The deformation behavior predicted by the model thus matches the real behavior. This is why the wall displacement prediction curves are close to the field measurements at early stages.

When excavation advances deeper, *i.e.*, intermediate to final stages, the unloading force was large enough to cause the stress state of the soil to be in the plastic state, *i.e.*, path A-B-C-E and relative large deformation occurs (Fig. 7). However, with analysis using the MCC model, the stress state predicted from the model may be still inside the MCC yield surface. Hence, the predicted wall displacements are smaller than the field measurements.

Figure 6 also shows that the predicted surface settlements are much smaller than the field measurements for the soil near the wall but larger than the field measurements for the soil far away from the wall. This is attributed to the fact that the small strain characteristics are not considered in the MCC model and the soil stiffness for the soil far away from the wall are underestimated in the model.

In order to get better analysis results, the parameter κ of the soils should be adjusted because the soil in front of the wall is subject to unloading force and the parameter κ is directly related to the behavior of the soil subject to unloading force. Considering that use of the MCC model may cause the normally consolidated soil in front the wall to be in the plastic state while the overconsolidated soil may be still in the elastic state, we therefore raise

Table 3 Input parameters of undrained material for the MCC model

Depth (m)	γ_t (kN/m^3)	M	υ_{ur}	κ/λ
0 ~ 5.6	18.25	1.2	0.2	0.09
8 ~ 12	18.15	1.16	0.2	0.1
12 ~ 33	18.15	1.16	0.2	0.1 ~ 0.15
35 ~ 37.5	19.13	1.2	0.2	0.14

Note: (1) e, λ and κ are also the input parameters and obtained directly from Figs. 2 and 3, respectively
(2) κ/λ is an not an input value, but it is for reference

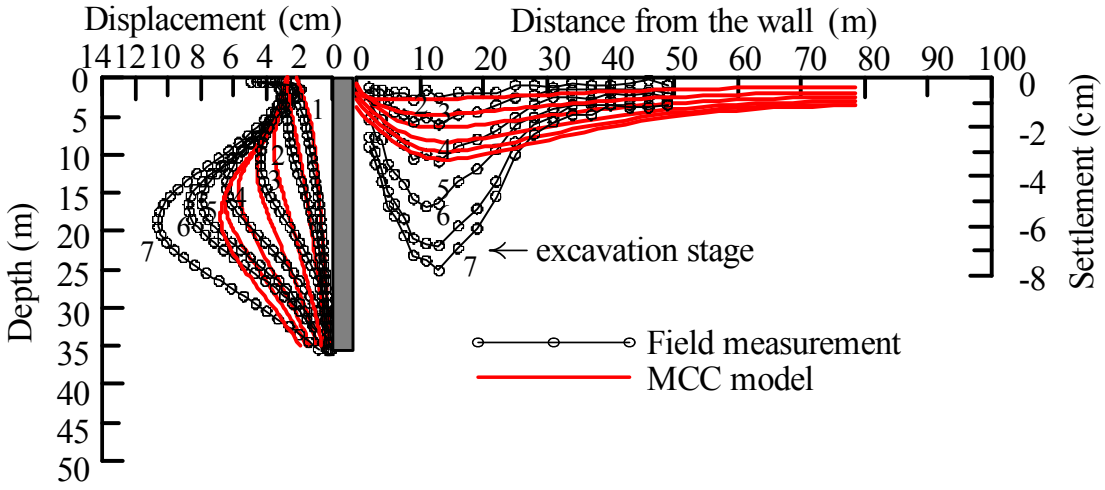

Fig. 6 The comparison of measured wall displacement and ground settlement profile with predicted using MCC model (real soil parameter)

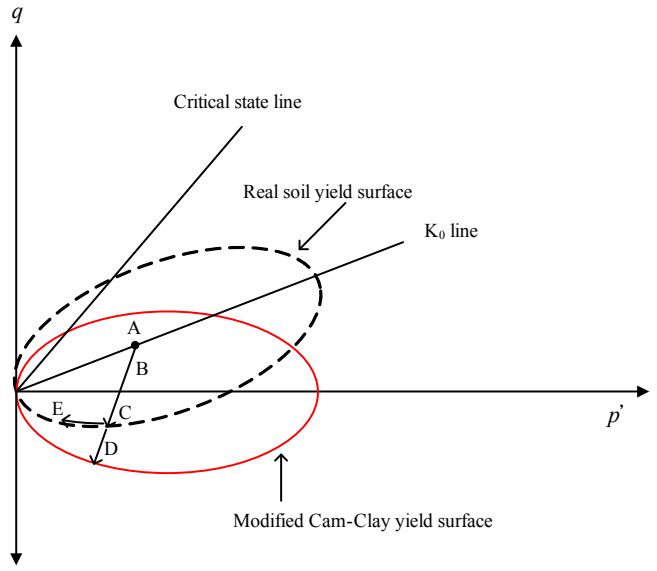

Fig. 7 Relationship of stress path in modified Cam-Clay yield surface and real soil yield surface

the κ/λ ratio for the normally consolidated clay, at the depth of 12 ~ 37.5 m, to be 0.2 while the κ/λ ratio for the overconsolidated soil, at the depth of 0 to 12 m, remains unchanged. The rest of the input parameters remain to be unchanged. Table 4 lists the adjusted input parameters of the MCC model. Figure 8 shows the comparison of measured wall displacements and those predicted using the MCC model with the adjusted parameters, as mentioned above. As shown in the figure, the predicted wall displacements fit the field measurements quite well for stages 4, 5 and 6 but not for the final stage. The κ/λ = 0.2 is still unable to make the predicted wall deflections fit the field measurements for the final stage.

Figure 9 shows the comparison of the predicted wall displacements with those using the MCC model with ratio of κ/λ = 0.25 for the normally consolidated soil. Note that the κ/λ ratio for overconsolidated soil and the other parameters are also unchanged. As shown in the figure, the predicted wall displacements fit the field measurement quite well for the final stage. However, the predicted wall displacements for the other stages are larger than the field measurements. This is because reduction of the soil elastic stiffness does not cause the number of the soil elements in the front of the wall that are in the plastic deformation largely increase and therefore the wall displacements at the stages 6 and 7 are fairly close to each other. The predicted wall displacement at the final stage close to the field measurement is mainly due to the reduction of soil stiffness rather than the soil in the plastic state.

Both Figs. 8 and 9 show that the surface settlements predicted from the model are still far from the field measurements even though the soil stiffness is reduced. To improve the prediction accuracy in surface settlement, small strain characteristics of the soil should be taken into account.

3.2 The Hardening Soil Model

The Hardening Soil model (Schanz *et al*. 1999), abbreviated as HS model, is a true second order model for soils in general (soft soil as well as harder types of soil). The model involves frictional hardening characteristics to model plastic shear strain in deviatoric loading, and cap hardening characteristics to model plastic volumetric strain in primary compression. Failure is defined by means of the Mohr-Coulomb failure criterion. The hardening soil model requires 9 parameters, *i.e.*, three reference stiffness parameters (E_{50}^{ref} for triaxial compression, E_{ur}^{ref} for triaxial unloading/reloading or elastic Young's modulus, E_{oed}^{ref} for oedometer loading) at a reference stress level p^{ref}, a power, m, for the stress dependent stiffness formulation, the pure elastic Poisson's ratio or unloading/reloading Poisson's ratio, υ_{ur}, the Mohr-Coulomb strength parameters (ϕ, c), the K_0-value in primary one-dimensional compression (K_0^{nc}), and failure ratio, R_f, which determines the strain level to failure.

For stiffness parameters, the pure elastic or unloading/reloading Young's modulus, E_{ur}^{ref}, can be obtained according to Eq. (3). According to Calvello and Finno (2004), E_{50}^{ref} = 1/3 E_{ur}^{ref} and E_{oed}^{ref} = 0.7 E_{50}^{ref}. The power parameter, m, is equal to one for soft clay soil and the υ_{ur} = 0.2, as suggested in the PLAXIS manual. The rest of the soil parameters are exactly the same as those adopted in the MCC model.

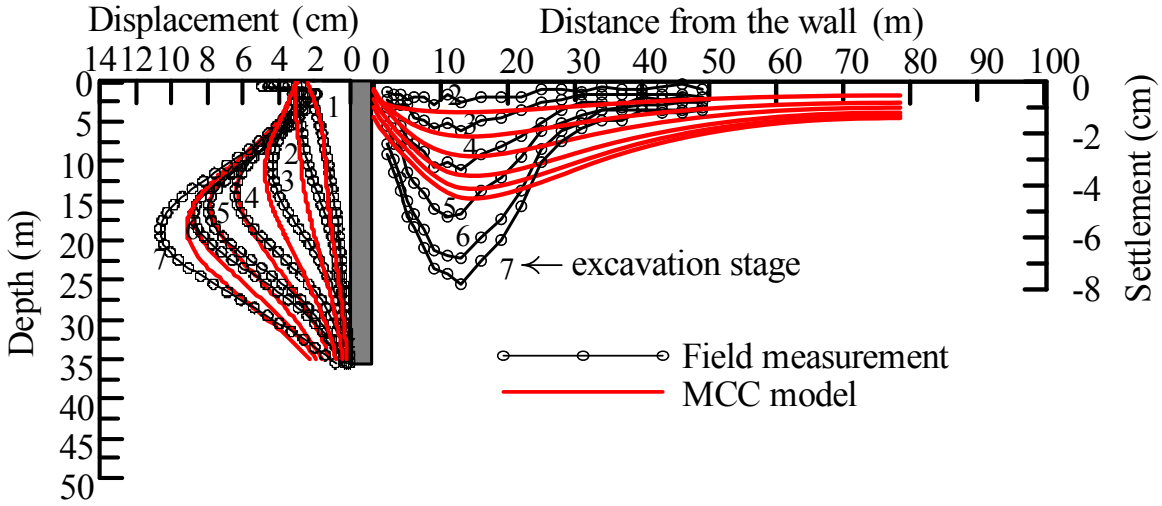

Fig. 8 The comparison of measured wall displacement and ground settlement profile with predicted using MCC model (adjusted parameter, κ/λ = 0.2)

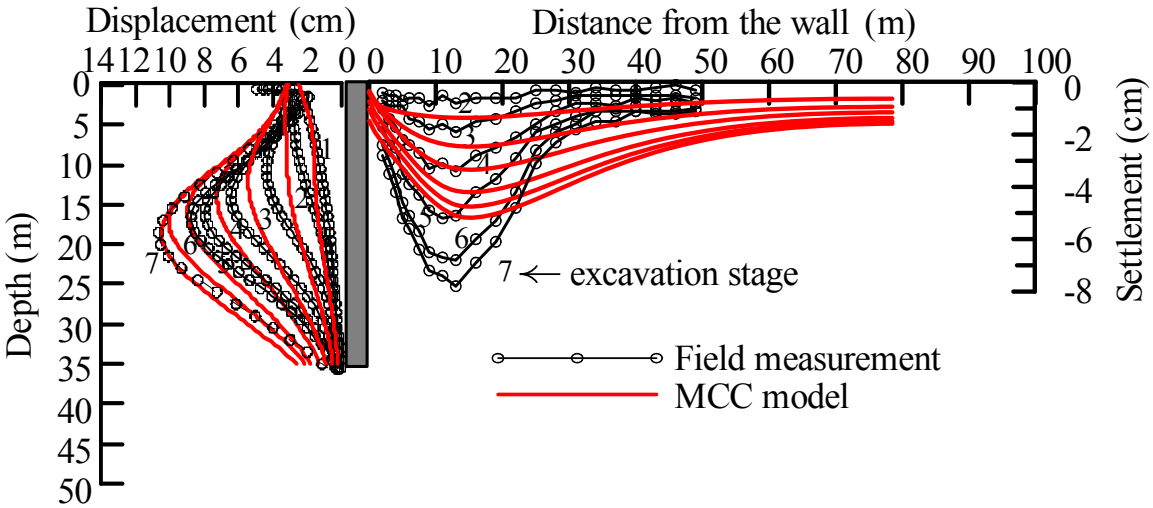

Fig. 9 The comparison of measured wall displacement and ground settlement profile with predicted using MCC model (adjusted parameter, κ/λ = 0.25)

Table 4 Adjusted input parameters of undrained material for the MCC model

Depth (m)	γ_t (kN/m^3)	M	κ	υ_{ur}	κ/λ
0 ~ 5.6	18.25	1.2	–	0.2	0.09
8 ~ 12	18.15	1.16		0.2	0.1
12 ~ 33	18.15	1.16	0.2λ	0.2	0.2
35 ~ 37.5	19.13	1.2	0.2λ	0.2	0.2

Note:(1) e an λ are also the input parameters and obtained directly from Figs. 2 and 3, respectively; (2) κ for the soil at a depth of 0 ~ 12 m is adopted from Fig. 3 and for the soil below 12 m is estimated to be 0.2λ; (3) κ/λ is an not an input value, but it is for reference

Figure 10 shows the comparison of the measured wall displacements and those predicted by the HS model. As shown in the figure, the wall displacement at the final stage predicted from the model is generally close to the field measurement though the wall displacement a depths of 10 m below the surface is slightly greater than the field measurement. The predicted wall displacements for the other stages are generally larger than those from field measurement. This implies that the HS model may be suitable for the analysis of geotechnical structures near the limiting state. When most of the soil in geotechnical structure is far from the limiting or failure state, the HS model yields a relatively large prediction result.

Figure 10 also shows the comparison of measured surface settlements and those predicted from the HS model. Compared with the MCC model, the HS model gives better prediction results. However, the settlements of soil far from the wall predicted from the model are still larger than the field measurements. As mentioned in the preceding section, small strain characteristics of the soil should be taken into account in the model to obtain better prediction results.

3.3 The Hardening Soil Small Model

The hardening soil small model, abbreviated as HS small model, evolves from the hardening soil model with the consideration of small strain characteristics of soil. In the HS small model, two additional parameters are required in addition to those in the hardening soil model. The two additional parameters are the reference shear modulus at small strain (G_0^{ref}) and shear strain ($\gamma_{0.7}$) at which the secant shear modulus equal to 0.7 G_0^{ref}. In the analysis of TNEC case history, the reference shear modulus at small strain (G_0^{ref}) is converted from the Young's modulus at small strain, which was obtained from the bender element test and will be discussed in the USC model (Section 3.5). The $\gamma_{0.7}$ can be estimated following the suggestion in the PLAXIS manual as

$$\gamma_{0.7} = \frac{1}{9G_0}\left[2c'(1+\cos 2\phi') - \sigma_1'(1+K_0)\sin 2\phi'\right] \tag{5}$$

where K_0 is the coefficient of lateral earth pressure at rest and σ_1' is the effective vertical stress.

Figure 11 shows the analysis results using the model with $\gamma_{0.7}$ estimated from Eq. (5). Both the wall deflections and surface settlements computed from the HS small model are much less than those from the field measurements. Since the value of G_0^{ref} is relatively reliable because it is converted from the test data, estimation of $\gamma_{0.7}$ from Eq. (5) should be modified.

Instead of using Eq. (5), we assume $\gamma_{0.7} = 10^{-5}$ because the strain of 10^{-5} usually falls into the category of small strain. We treat 10^{-5} as a threshold value of small strain. Figure 12 shows the analysis results using the model with $\gamma_{0.7} = 10^{-5}$. Compared Figure 12 with Figure 11, use of $\gamma_{0.7} = 10^{-5}$ seems to give a better prediction. Compared with the results by the hardening soil model (Fig. 10), the HS small model does not have a good effect in improving the analysis accuracy. The wall displacements predicted from the HS small model for all stages are slightly larger than those from field measurement. The HS small model gives slightly better prediction in surface settlements though the prediction results are still far from the field measurements.

The idea of HS small model is to consider small strain properties by introducing a threshold shear strain, $\gamma_{0.7}$, which is the shear strain when the secant shear modulus, G, is reduced to 70% of G_0. As shown in Figs. 11 and 12, use of stress level of 0.7, as a threshold shear strain or HS small model does not seem enough to improve the analysis accuracy.

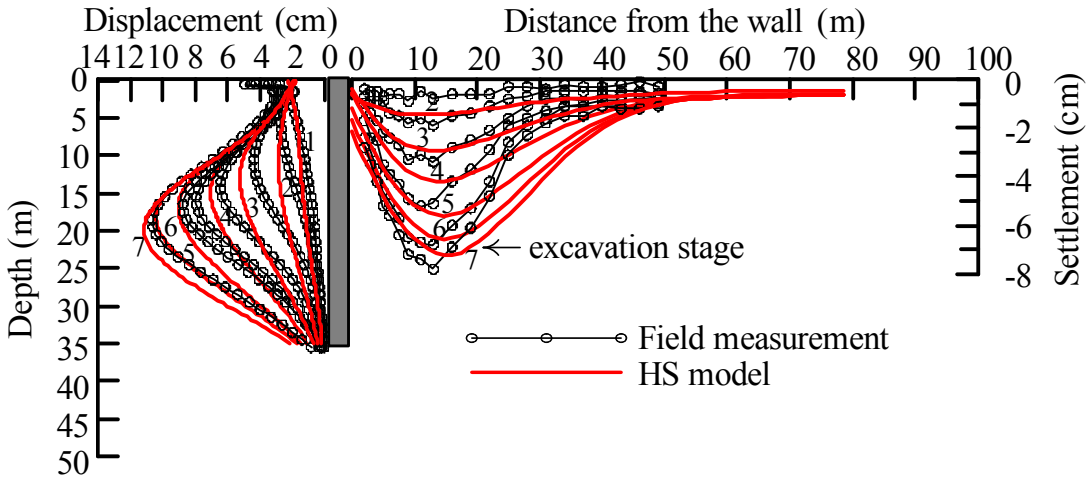

Fig. 10 The comparison of measured wall displacement and ground settlement profile with predicted using HS model

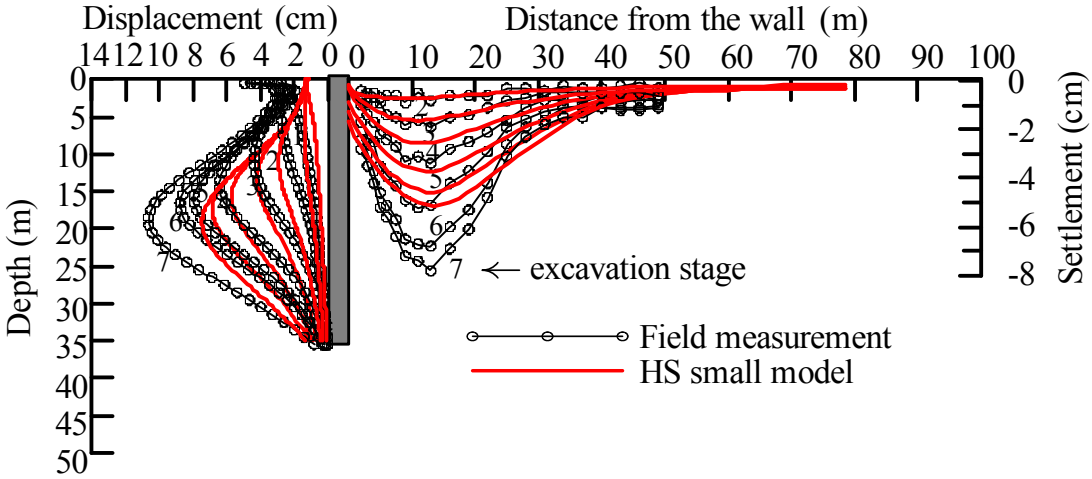

Fig. 11 The comparison of measured wall displacement and ground settlement profile with predicted using HS small model ($\gamma_{0.7}$ evaluated from Eq. (5))

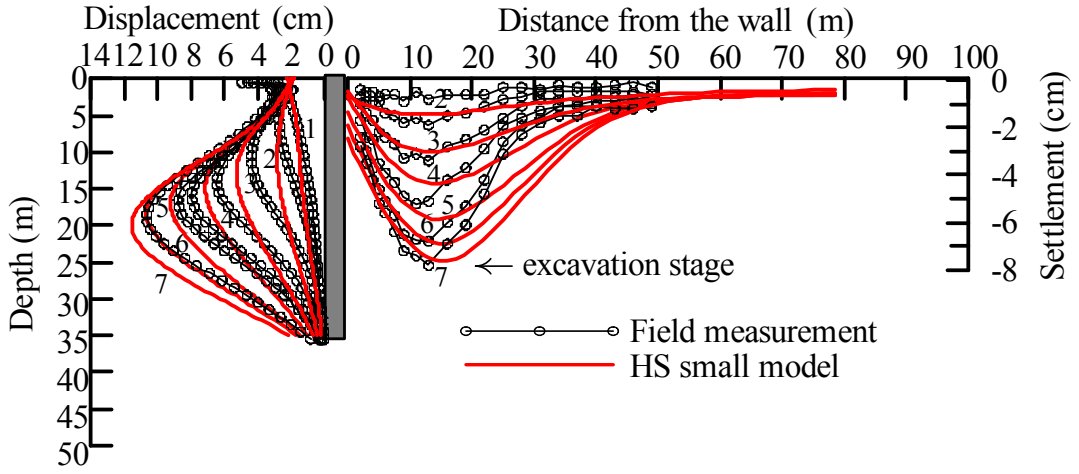

Fig. 12 The comparison of measured wall displacement and ground settlement profile with predicted using HS small model ($\gamma_{0.7}$ equal to 10^{-5})

3.4 The $\phi = 0$ Mohr-Coulomb Model

The Mohr-Coulomb model is an elastic perfectly-plastic model and in fact, a combination of Hooke's law and the generalized form of Coulomb's failure criterion. The model involves four parameters, namely the two pseudo-elastic parameters from Hooke's law (Young's modulus, E, and Poisson's ratio, υ), and the two parameters from Coulomb's failure criterion (the friction angle, ϕ, and cohesion intercept, c).

With the total stress analysis, the undrained Poisson's ratio, υ_u, should be equal to 0.5 for the saturated clay under the undrained condition. The cohesion intercept should be equal to undrained shear strength, *i.e.*, $c = S_u$ and the friction angle is equal to 0. In this study, the undrained shear strength from the field vane shear test is adopted for analysis (Fig. 4). The undrained elastic Young's modulus, E_u, can be determined based on PI and OCR following the method proposed by Chang and Abas (1980), as shown in Fig. 12. The lower bound values of the relational curves in Fig. 13 are adopted to estimate E_u. Table 5 lists the input parameters of undrained material for the Mohr-Coulomb model. Figure 14 shows that the predicted wall displacements and surface settlements are much smaller than those from field measurements. The relationship established by Chang and Abas (1980) is obviously not suitable for the $\phi = 0$ Mohr-Coulomb model though the Chang and Abas' method has been used to estimate the undrained Young's modulus in Duncan-Chang model in the past (Ou and Lai 1994).

Since Chang and Abas' (1980) method does not give a good result for wall displacement and surface settlement, back analysis on the basis of wall displacement at the final stage is executed to obtain a reasonable value of the Young's modulus. It is found from parametric studies that a value of $E_u/S_u = 500$ could give reasonable wall displacements and the rest parameters are same as those presented in Fig. 14. Figure 15 shows the analysis result. As shown in Fig. 15, the predicted wall displacements for stages 4, 5, 6, 7 are quite close to field measurements. However, the general pattern of the wall displacement does not match the field measurements for stages 1, 2 and 3. It may be attributed to the fact that the total stress Mohr-Coulomb model is unable to predict actual soil behavior well. Even if the predicted wall displacement at the final stage can fit the field measurement, those at other stages are not predicted well. However, as long as the wall displacement at the final stage is concerned, use of $E_u/S_u = 500$ seems to give a reasonable prediction result. Similar to the MCC model and HS model, the Mohr-Coulomb model is unable to predict the surface settlement well.

3.5 The Undrained Soft Clay (USC) Model

The undrained soft clay model, abbreviated as the USC model, is a stress path dependent total stress model, which was developed with the following considerations (Hsieh *et al*. 2010):

(1) Variation of undrained shear strength with principal stress rotation
(2) Variation of Young's modulus with the increase of stress level
(3) High stiffness of soil at small strain
(4) Rational way to determine the undrained shear strength

The USC model is briefly introduced as the following:

Similar to Duncan and Chang's model (1970), the tangent Young's modulus (E_t) can be derived as

$$E_t = E_{ur}(1 - R_f\ SL)^2 \tag{6}$$

where R_f is the failure ratio; SL, the stress level, is the ratio of increment of deviatoric stress at the current stress state to the increment of deviatoric stress at the failure state; E_{ur} is the pure elastic Young's modulus or unloading/reloading Young's modulus.

Table 5 Input parameters of undrained material, estimated from Chang and Abas (1980), for the Mohr-Coulomb model

Depth (m)	γ_t (kN/m^3)	$S_u^{(1)}$ (kPa)	E_u (kPa)	υ_u
0 ~ 5.6	18.25	–	2594 ~ 8261	0.495
8 ~ 33	18.15	–	26460 ~ 91773	0.495
35 ~ 37.5	19.13	–	135000	0.495

Note: (1) S_u is adopted from Fig. 4

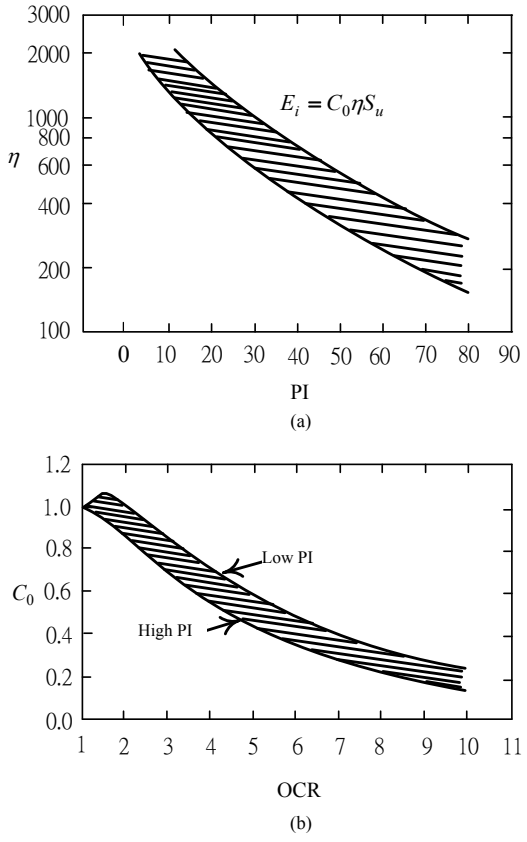

Fig. 13 Estimation of Initial Tangent Modulus proposed by Chang and Abas (1980)

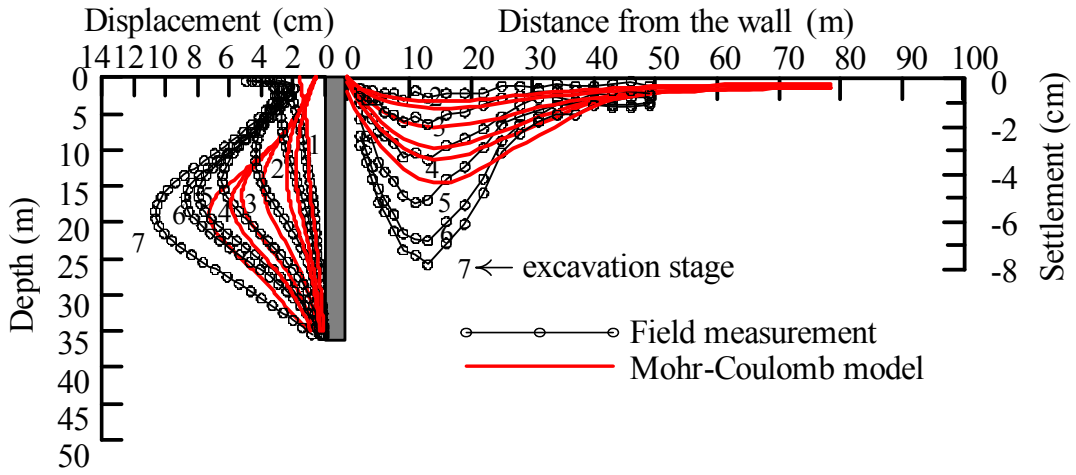

Fig. 14 The comparison of measured wall displacement and ground settlement profile with predicted using $\phi = 0$ Mohr-Coulomb model (Chang and Abas, 1980)

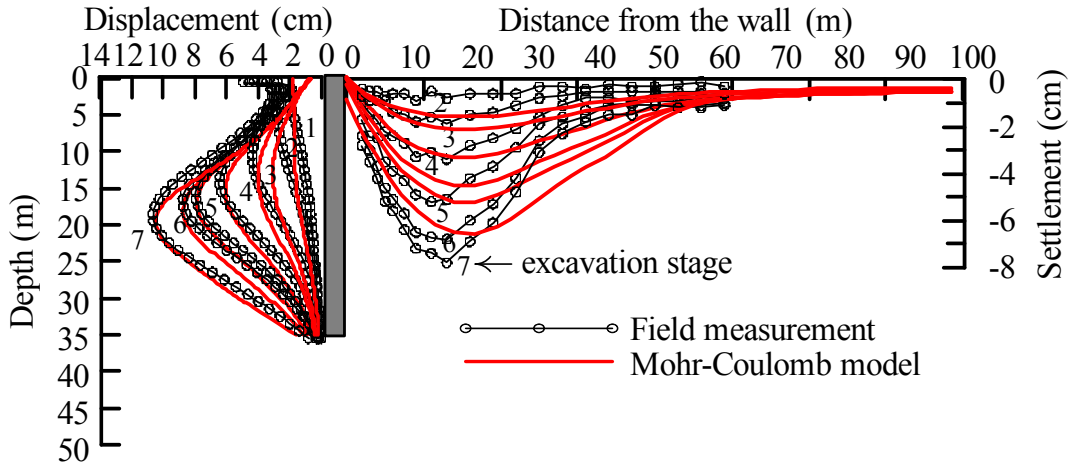

Fig. 15 The comparison of measured wall displacement and ground settlement profile with predicted using $\phi = 0$ Mohr-Coulomb model (back analysis)

The pure elastic Young's modulus or unloading/reloading Young's modulus, E_{ur}, should degrade, from the range of small strain, with the increase of strain or stress level due to the development of pore water pressure (Fig. 16). The degraded Young's modulus is assumed to follow a hyperbolic function as

$$\frac{E_{ur}}{E_i} = 1 - \frac{SL - SL_i}{m + n(SL - SL_i)} \tag{7}$$

where m and n are the degradation parameters relative to the stress level; E_i is the initial Young's modulus or the Young's modulus at small strain; SL_i is the stress level corresponding to the threshold value of the small strain or the initial yield strain.

An elastic surface, ES, is defined to represent the small strain characteristics for the state of stress inside the elastic surface. The elastic surface is expressed as (Fig. 17):

$$ES = \frac{(q - q_0)^2 + V^2}{\left(\frac{\delta\sigma_{di}}{2s_{uc}}\right)^2} - 1 = 0 \tag{8}$$

where q is the normalized deviator stress in the x-y plane, $q = [(\sigma_y - \sigma_x)/2]/s_{uc}$; σ_y is the vertical total stress; σ_x is the horizontal total stress; s_{uc} is the undrained shear strength obtained from the triaxial CK_0U-AC test; V is the normalized shear stress in the x-y plane, $V = \tau / s_{uc}$; τ is the shear stress on the x-y plane; q_0 is the q-value at the K_0 condition; $\delta\sigma_{di}$ is the change in deviator stress that corresponds to the threshold value of the elasto-plastic response or initial yield strain in the triaxial loading condition and its value is equal to $E_i \varepsilon_i$; and ε_i is the threshold value of the small strain or initial yield strain.

When the state of stress is within the elastic surface, the Young's modulus at small strain is treated as the initial Young's modulus (E_i) or the maximum unloading/reloading Young's modulus, $E_{ur,\max}$.

The USC model adopts the following function as the yield function to differentiate the stress states between the unloading/reloading state and primary state.

$$\left[q - q_c \; SL - q_0(1 - SL)\right]^2 + V^2 = \lambda^2 R^2 \tag{9}$$

where q_f is the q value at the failure condition; q_c is the q value at the center of the failure surface, $q_c = (1 - K_s)/2$; K_s is the anisotropic undrained strength ratio, $K_s = s_{ue}/s_{uc}$; s_{ue} is the undrained shear strength from the CK_0U–AC test ; R is the radius of the failure surface, $R = [(3K_s + 1)(K_s + 3)/12]^{1/2}$; λ is a parameter that identifies the size of the yield surface, *i.e.*, λR is the radius of the yield surface; and SL is the stress level at the current stress state.

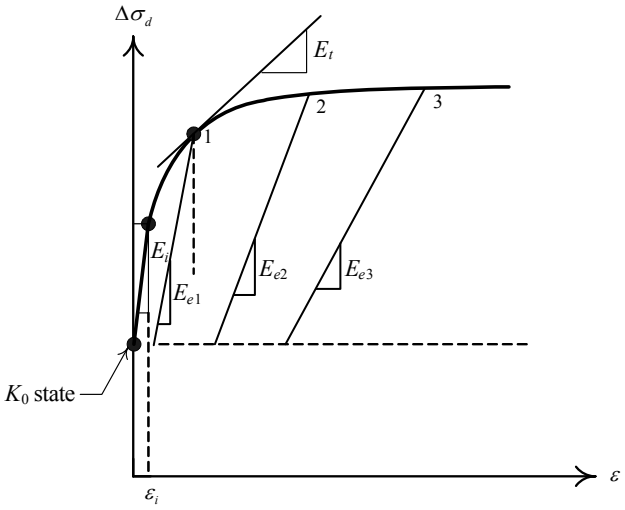

Fig. 16 Schematic description of the degradation of the elastic Young's modulus

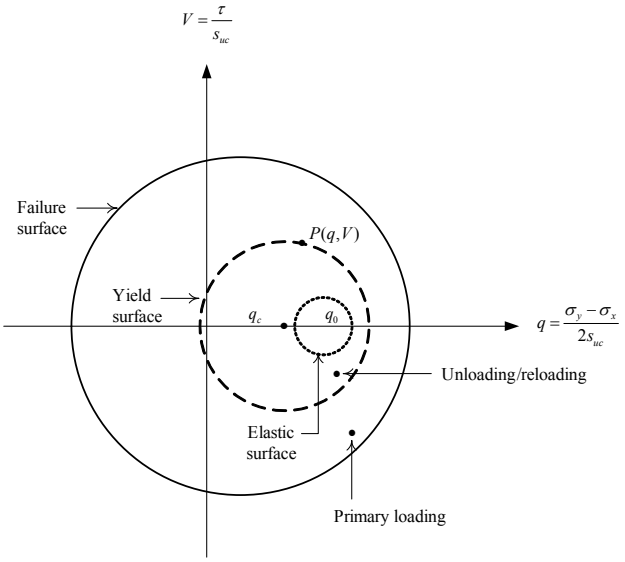

Fig. 17 Relationship among elastic surface, yield surface and failure surface

In the analysis, when the state of stress is within the elastic surface, the Young's modulus (E_i) at small strain should be used for analysis, *i.e.*, $E = E_i$. When the state of stress is outside of the elastic surface and the current stress level is smaller than the past maximum stress level, the soil is in the unloading/reloading state, and the pure elastic or unloading/reloading Young's modulus, E_{ur}, as calculated from Eq. (6) at the current stress state should be employed.

Figure 17 also displays the relationship between elastic surface, yield surface and the failure surface.

Under the plane strain condition, the undrained shear strength ($s_{u\beta-ps}$), oriented at an angle β to the vertical line, can be estimated by the following equation, which was derived by Hsieh *et al*. (2008) as follow

$$s_{u\beta-ps} = \left[\sqrt{R^2 - (q_c \sin 2\beta)^2} + q_c \cos 2\beta\right] s_{uc} \tag{10}$$

Details of the USC model can refer Hsieh *et al*. (2010). The input parameters for the USC model are anisotropic undrained ratio (K_s), undrained shear strength (S_{uc}) from the triaxial CK_0U-AC test, Young's modulus at small strain (E_i), failure ratio (R_f), degradation parameters (m and n), Poisson's ratio (υ). Table 6 lists the parameters of the USC model, their physical meaning and methods to obtain them.

Table 7 lists the parameters used for analysis of the TNEC case history. Figure 18 compares the wall displacements from field measurement with those predicted from the USC model, which indicates that the computed wall deflections for all stages agree well with the field observations. The development of the wall deflection shape with the construction sequence and the location of the maximum wall deflection computed from the model are also very close to those observed in field observation. The computed surface settlements are also in good agreement with the observed settlements. The location of the maximum surface settlement computed from the model is almost the same as that from field observation. The USC model predicts both wall deflection and surface settlement well.

In general effective stress models are preferable by geotechnical scientists rather than total stress models because the former meets the effective stress principle. Though the USC model is a total stress based model, it can yield an accurate prediction in both wall deflection and surface settlement. The main reason may be due to the fact that the model is a stress path dependent model, which is able to consider the behaviour of the soil for various stress paths.

4. CONCLUSIONS

The conclusions of this study are as following:

1. With the modified Cam Clay model, the wall displacements and ground settlements predicted using the real soil parameters are much smaller than field measurements. To make the predicted wall displacements fit the field measurements, the κ/λ ratio for the normally consolidated soil should be increased up to 0.25 while the κ/λ ratio for the overconsolidated soil should be kept unchanged. However, such an adjustment for the κ/λ ratio only makes the predicted wall displacements to fit the field measurements for the final stage of excavation, in which the stress state of soils are close to the limiting condition. The predicted wall displacements for the other stages are generally larger than the field measurements. The predicted surface settlements for all stages are far from the field measurements because small strain characteristics of soil are not taken into account in the model.
2. With the hardening soil model, the predicted wall displacement is generally close to the field measurement for the final stage of excavation but larger than the field measurement for other stages of excavation. Compared with the modified Camclay model, the hardening soil model gives better prediction in surface settlement but still far from the field measurements.
3. Basically the hardening soil small strain model give almost the same prediction in wall displacement as the hardening soil model and slight improvement of prediction in surface settlement though small strain characteristics are implemented in the model.
4. With the ϕ = 0 Mohr-Coulomb model, a common total stress model, a value of $E_u / S_u = 500$, which is derived from the back analysis, can make the predicted wall displacements fit the field measurements for intermediate to the final stages. The general pattern of the wall displacement predicted using the

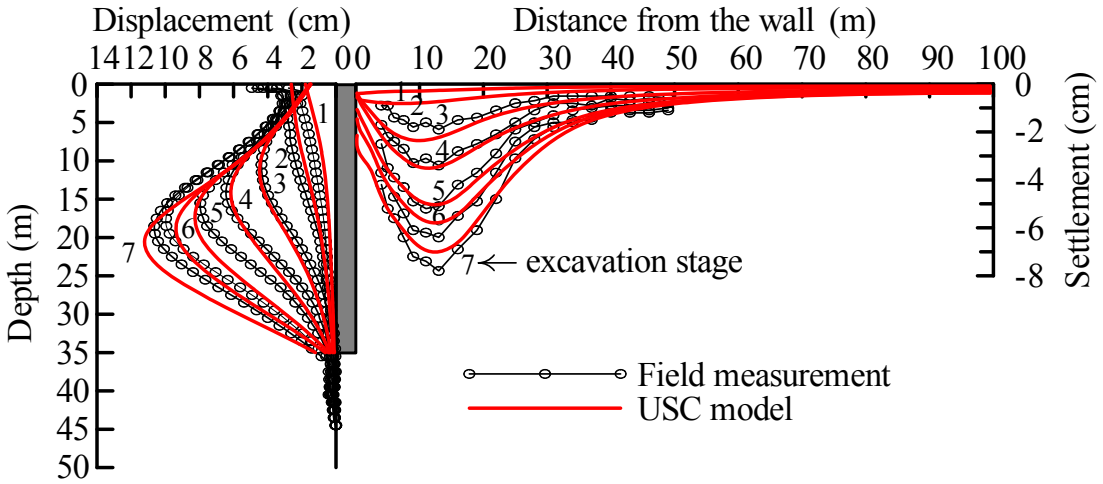

Fig. 18 The comparison of measured wall displacement and ground settlement profile with predicted using USC model

Table 6 Parameters for describing the USC model and their physical meanings

Parameters	Definition or physical meaning	Methods to obtain parameters
s_{uc}	Undrained shear strength under the triaxial condition (compressive mode)	Triaxial CK_0U-AC test
E_i	Initial Young's modulus or the maximum elastic Young's modulus	Bender element tests or small strain test at strain about $10^{-5} \sim 10^{-6}$
R_f	Failure ratio	Same as Duncan and Chang model, $R_f \approx 0.9$ for soft clay
K_s	Anisotropic strength ratio, $K_s = s_{ue} / s_{uc}$; s_{ue} is the undrained shear strength under the triaxial condition (extension mode)	Triaxial CK_0U-AC and CK_0U-AE tests
m, n	Stiffness degradation parameters, which reflect the variation of pore water pressure generation with strain	Multiple unloading and reloading test

Table 7 Input parameters of undrained material for the USC model

Depth (m)	γ_t (kN/m^3)	s_{uc} / σ'_v	E_i / s_{uc}	R_f	m	n	K_s	υ
0 ~ 5.6	18.25	0.32	2100	0.9	0.225	1.299	0.75	0.495
8 ~ 33	18.15	0.34	2100	0.9	0.225	1.299	0.75	0.495
35 ~ 37.5	19.13	0.36	2100	0.9	0.225	1.299	0.75	0.495

model is far from the field measurement for early stages. This implies that the $\phi = 0$ Mohr-Coulomb model is unable to predict the stress state for all loading conditions.

5. The USC model is a stress path dependent total stress model, which requires seven parameters to describe soil behavior. All of the parameters can be obtained from conventional soil tests. The model can result in a very good prediction for both wall displacements and surface settlements for all stages of excavation.

REFERENCES

Benz, T., Vermeer, P. A., and Schwab, R. (2009). "A small-strain overlay model." *International Journal for Numerical and Analytical Methods in Geomechanics*, **33**, 25-44.

Burland, J. B. (1965). "The yielding and dilation of clay." *Geotechnique*, **15**, 211-214.

Calvello, M. and Finno, R. (2004). "Selecting parameters to optimize in model calibration by inverse analysis." *Computer and Geotechnics,* **31**, 410-424.

Chang, C. S. and Abas, M. H. B. (1980). "Deformation analysis for braced excavation in clay." *Proceedings of the Symposium on Limit Equilibrium, Plasticity and Generalized Stress Strain Applications in Geotechnical Engineering*, ASCE, Hollywood, Florida, 205-225.

Duncan, J. M. and Chang, C. Y. (1970). "Nonlinear analysis of stress and strain in soils." *Journal of the Soil Mechanics and Foundations Division,* ASCE, **96**, 637-659.

Hashash, Y. M. A. and Whittle, A. J. (1996). "Ground movement prediction for deep excavations in soft clay." *Journal of Geotechnical Engineering*, ASCE, **122**, 474-486.

Hsieh, P. G., Ou, C. Y., and Liu, H. T. (2008). "Basal heave analysis of excavations with consideration of anisotropic undrained strength of clay." *Canadian Geotechnical Journal*, **45**, 788-799.

Hsieh, P. G., Ou, C. Y., and Lim, A. (2010). "Use of the total stress undrained model to the analysis of deep excavation." *Proceedings of the 17th Southeast Asian Geotechnocal Conference*, Taipei, Taiwan.

Ou, C. Y. (2006). *Deep Excavation: Theory and Practice*. Taylor and Francis, Netherlands.

Ou, C. Y. and Lai, C. H. (1994), "Finite element analysis of deep excavation in layered sandy and clayey soil deposits." *Canadian Geotechnical Journal*, **31**, 204-214.

Ou, C. Y., Liao, J. T., and Cheng, W. L. (2000). "Building response and ground movements induced by a deep excavation." *Geotechnique*, **50**, 209-220.

Ou, C. Y., Liao, J. T., and Lin, H. D. (1998). "Performance of diaphragm wall constructed using top-down method." *Journal of Geotechnical Engineering and Geoenvironmental Engineering,* **124**, 798-808.

Ou, C. Y., Shiau, B. Y., and Wang, I. W. (2000), Three-dimensional deformation behavior of the TNEC excavation case history, *Canadian Geotechnical Journal*, **37**, 438-448.

Pestana, J. M. and Whittle, A. J. (1999). "Formulation of a unified constitutive model for clays and sands." *International Journal for Numerical and Analytical Methods in Geomechanics*, **23**, 1215-1243.

Prevost, J. H. (1979). "Undrained shear tests on clay." *Journal of the Geotechnical Engineering Division,* ASCE, **105**, 49-64.

Schanz, T., Vermeer, P. A., and Bonnier, P. G. (1999). "The hardening soil model: Formulation and verification." *Beyond 2000 in Computational Geotechnics – 10 years PLAXIS*. Balkema, Rotterdam.

Schofield, A. and Wroth, P. (1968). *Critical State Soil Mechanics*, McGraw-Hill, London.

Teng, F. C. (2010). Personal file.